

Neutron Number Asymmetry in Proton Decay Momentum

Yang I Pachankis

Universal Life Church, USA

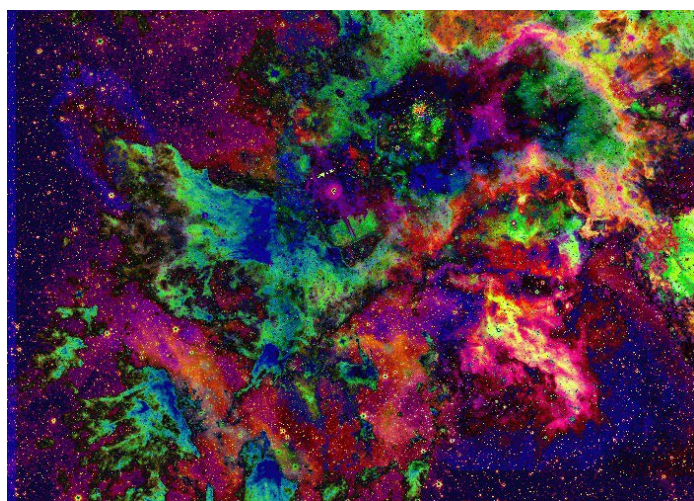
*Corresponding author: Yang I Pachankis, Universal Life Church, USA

Submitted: 11 Nov 2022 Accepted: 18 Nov 2022 Published: 23 Nov 2022

Citation: Yang I Pachankis (2022). Neutron Number Asymmetry in Proton Decay Momentum . J of Agri Earth & Environmental Sciences, 1(1), 01-09.

Abstract

The cosmic censorship hypothesis put a threshold on the observable universe with the order of magnitude in the visible spectrum and space-time singularity. The research put the question into the scope of chemical cosmology in local universe cases of black hole and white hole thermonuclear binding. The research adopted a controlled group data experiment with the NASA multi-mission all-spectrum space telescopes for thermonuclear chemical recombination in quantum, and an experimental group with Harvard-Smithsonian Micro Observatory in observational cosmology testing. References on the controlled group were taken on the data products of 2Mass, WISE, and neoWISE missions in critical mass behaviors behind the information conundrum. The controlled group experiment ended with the result on the presence of antimatter Van der Waals force behind the plausible cause of the cosmic censorship hypothesis, and the experimental group included one result on the thermonuclear induction to the high frequency Doppler Shift to the annihilating dark matter momentum. The research concludes that the wrapping of time can be applied to the wrapping of space itself for a thermal arrow of time in general relativity with the SI Unit of definition, paving a cosmological foundation to quantum gravity.



Explosive Energy Phenomenon on Carina Nebula from 2022 NASA Data Challenge

Introduction

The phenomenon of Many-Worlds Interpretation for quantum mechanics put the uncertainty principle in statistical probabilities in the wave function. With the recombination of local universe through quasi-particles considered as products from local astrochemical radiations the experiment confirmed the thermonuclear binding of a black hole and a white hole with a Kerr-Newman

case and the fifth cosmic force [1-4]. The question on the gravitational frame's non-imaging led to a refocus on antimatter electromagnetism and possible Van der Waals force equivalence therein with the quadruple momentum [5]. The analysis on the positive null result in the controlled group contributes to the dark energy phenomenon interpretation from a higher order of force with effects in electrochemical observation revealed as high frequency Doppler Shift tested in the experiment group result [6,7]. The research proposes that the warping of time on cosmological scale is necessary with the presence of electrolysis effects affecting the SI unit definition of time, solving the thermodynamic conundrum in the physical cosmological interpretations and advancing the holographic principle in quantum gravity [8-11].

While photon catalysis has been used in quantum mechanical experiments and particle physics experiments, the research method of particle-filtering adopted to the nuclear spectra empirically analyzed the multi-spectral thermonuclear reactions from respective angular momenta [7,12]. Hazard report was immediately authored upon the cross-referenced results of the controlled and experimental groups, which served as evidence for communication with the International Criminal Court and International Court of Justice [6,13]. With the confirmation of the fifth cosmic force from the experimental group the article furthers the input on the observations and analysis of the antimatter Van der Waals force behavior and interactions with the electromagnetic spectrum in the methods [4,14].

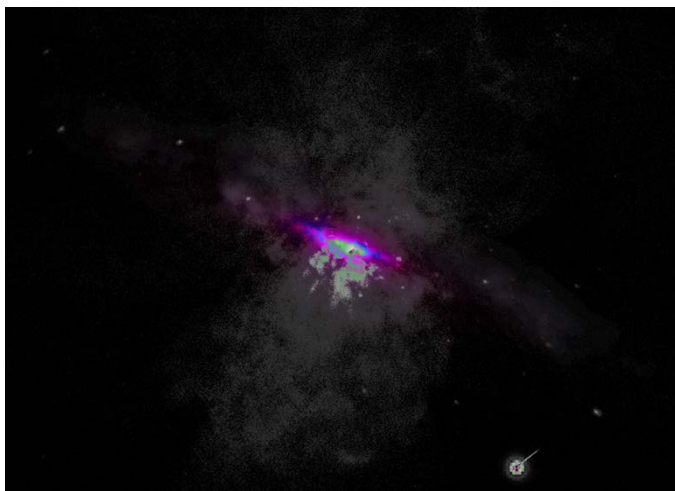


Figure 1: The decay burst on NGC 3034 ring singularity in confined thermonuclear dipole shift [3].

Methods

Physical laws were believed to have ceased working upon a black hole event horizon. The theoretical method treated the SI unit definition of time to the arrows Pachankis summarized" can be bidirectional in thermodynamics with regard to special relativity". It means that epistemically, the observers are in space but not in time [15,16]. Therefore, time in the local universe can be objectively re-constructed by the presence of matter & antimatter thereof. From the singularity onward, the controlled group experiment attempted to construe the geodesics of the anticipated black hole and white hole from the angular momenta by the particle-filtering process in controlled wettability, sorting the surface plasmas from the wave function, seen in figure 1 [12]. The method of nuclear spectra recombination is repeatedly tested in the experimental groups and later multi-mission group [7,17].

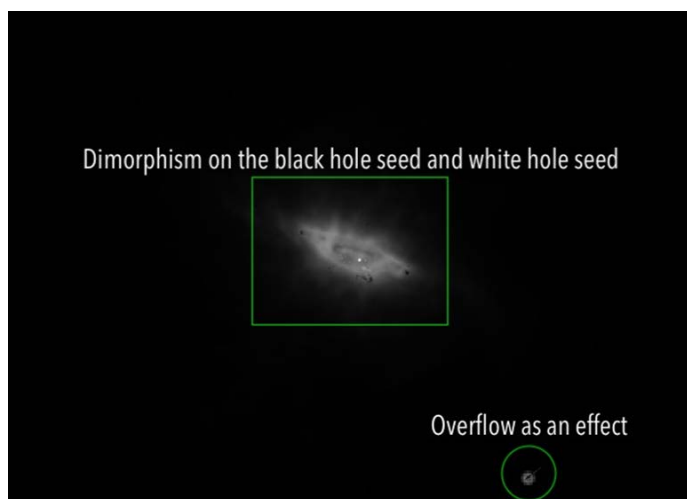


Figure 2: Annotated collision momentum of the black hole seed and white hole seed on the ring singularity with the phenomenology described by Forrington as" Magnetosphere Eternally Collapsing Object (MECO)" [18,19].

The initial research followed an electrolysis induction from the weak-force slit caused by the thermonuclear explosive astrophysical process recovering the traditionally perceived electroweak force ring singularity on the Kerr-Newman type black

hole, with the notice on the strong force being influenced by the antimatter presence [12,20]. By the notice on the invariant Hawking points in the Chandra X-ray data behind the collision momentum dissected in figure 2 by dimorphism on the Chandra X-ray data pieces implying the cause for the formation of Hawking points [14,21]. The initial electrochemical wettability control on the ring singularity compensated for the limitations of pure physics isomorphic thinking with short circuit threshold, whereby Poincaré [22] described this as "... we ascertain besides that two of these systems can sometimes be discriminated from one another though indistinguishable from a third system ... with the manifold of these systems of impressions" forming "a physical continuum C". With the continuum, the circumnuclear descriptions [23] of the soft hair electrolysis touch point between the black hole seed and white hole seed [24] shapes the photon generation seen in figure 3.



Figure 3: Annotated off-focus processing on exotic metal-insulator formation on ring singularity on NGC 3034.

The phenomena of the Hawking points invariant in space relative to the local time of reference imply that the quadruple matter & antimatter electromagnetism observed in electrochemical slices is balanced by the short-range fifth cosmic force, plausibly with inter-point repulsive forces attracted together by the ring trajectory currents. The soft symmetry electric hair consisting of the cosmic censorship hypothesis in the Maxwell field thus consists of the weakly guarded catalyst point in the thermonuclear astrochemical reaction chains qualitatively reported [6,24]. The formation of the collision momentum from the asymptotic decay is conceptually drawn in figure 4. The thermal effects mean that the Hawking points' material origins may be from the conjunction of the black hole and the white hole around the fifth cosmic force [14].



Figure 4: The initial trajectories of seeds formation are asymmetrically intervened by the fifth cosmic force, breaking the "path of least resistance" [8,25].

A refined expression from Pachankis on the torque momentum in the local black hole and white hole in relation to the point of thermonuclear binding is expressed as [21]:

$$S^2 = \left(\frac{\omega r_i \vec{m}_{whs} \pi c^6}{h \nu m_{whs}} \right)^2 \left(\begin{array}{l} \omega = 2\pi \sqrt{\frac{e^- e^+ + \bar{e}^- \bar{e}^+}{2}} \\ \frac{m_{bhs} m_{whs}}{\omega^2} \geq \frac{E a^n c^2}{G} \end{array} \right) \quad (1)$$

The irradiation effect between the black hole and the white hole serves as exotic Bremsstrahlung between the black hole mass and white hole mass, and was processed with the opaque ground-based observation and the space-based infrared frames from SPITZER in figure 5. The cosmic source of dark energy, therefore, is closely related to the antimatter Van der Waals force behind the oscillation and possible other types in evolutionary developments organized in table 1

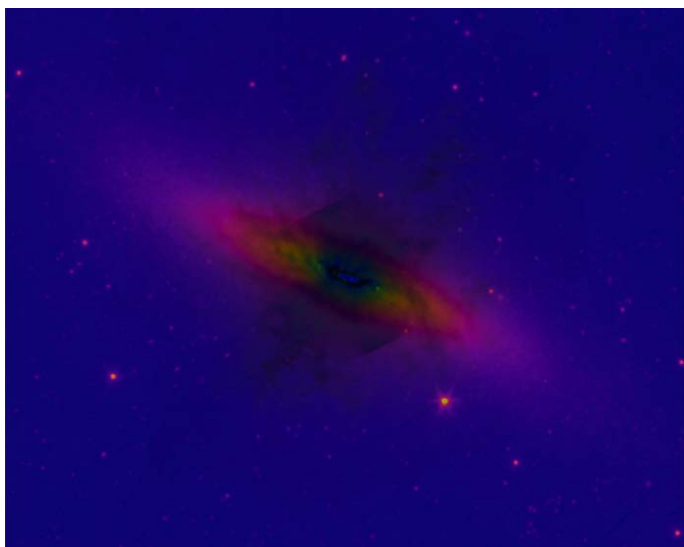


Figure 5: The quadruple electroweak nucleosynthesis on the ring singularity on NGC 3034.

Table 1: Observable electrolysis in black hole types

Non-charged	Charged
Schwarzschild ^a	Kerr-Newman ^b
Kerr ^b	Reissner-Nordström ^a

^a No spin; ^b With spin.

The types with no spin may have less observable physical causal locales than the types with spin, and the spin function may further irradiate white holes from their bonded black holes. This may also be contributed by the dominantly electromagnetic spectrum observation methods. Even though the quantum transitions are from black hole to white hole in discovery processes with the limitations and all possible paths in the holographic principle the cosmic origins may not follow such an order [4,26].

The original experiment was divided in the control group of data analysis and experiment group with observational cosmology [7]. In the control group, the black hole and white hole are treated as clocks in and of themselves in the local universe, and with the confirmation in the current developments in the 2Mass, WISE, and neoWISE missions the confidence on the thermal indicators led to the concurrent experiment group, treating earth as a clock with its inherent electromagnetic arrow overcoming the Van der Waals force's limitations set in instrumentation, with observational sequences in thermal arrows, defying the space-time geometry. Similar technique was adopted in the polymerization numerical analysis with the conjecture proposed Pachankis' "if the square root of n is irrational, n^{1/n} is irrational" [21]. The antimatter polymerization was performed on SAOImageDS9 with the presence being most prominent in the Chandra X-ray low and mid energy pieces and concentrated in high energy piece which made the topological numerical analysis into plasma analysis [27-29]. The dynamic relations between particles P[→] and singularity S[→] are expressed as:

$$\left(\begin{array}{l} \vec{P}_n \vec{S}_n \cong \vec{P}_{n-1} \vec{S}_{n-1} \\ |\vec{S}_{n-1} \Delta t_{n-1}| \tau_n \cong |\vec{P}_n \vec{S}_n| \end{array} \right) \quad (2)$$

When τ_n = 1 is considered, the numerical analysis can be simplified with Quaternion Multiplication dissecting the two masses from the multi-spectral data [30]. τ = Fv was presumed in analyzing empirically from data the relationship amongst singularity, the two masses, and the fifth cosmic force binding the two in the waves. Or in other words, the wave function in quantum particles can be morphed to the surface manifold of the local black hole and white hole pair [30]. Probability in the uncertainty principle is thus the influence observed in causal distribution of possibilities in the phenomenological world [31]. The analytical geometry, therefore, put particle and the concept of time on the same or equivalent footing in the special relativity based inductive experimental wetting.

The phenomenon of time frozen around a black hole with the SI unit definition of time is thus explained by the antimatter electromagnetism's influence to electrons in the observations both

in human biology and instrumentation from the consciousness in human anthropological evolution [19,16]. Combining the observational expression in equation 1 and the theoretical input on gravitation phenomenon from the singularity the mass of gravitational white hole to the angular momentum of the observer was expressed as [14,21]:

$$\left\{ \left| \frac{\Delta m_2}{m_2} \right| \geq \left| \frac{\vec{m}_{whs}}{m_{whs}} \right| \right\} \quad (3)$$

The impact from the Hawking points' formation from the fifth cosmic force conceptualized in figure 4 resonating the star systems seen in figure 5, connotes the Bekenstein-Hawking entropy formula in a galactic context:

$$\left\{ \frac{2ShEa^n}{\pi Akc} = \frac{m_B m_W}{\omega^2} \right\}. \quad (4)$$

Control Group

Kedem et al. acknowledged that 'condensed matter systems do not have Lorentz symmetry and an extra contribution to the Hamiltonian of the form $H_{\text{int}} = \vec{k} \cdot \vec{p}$ can appear', where 'k can become space-dependent' and 'the low energy, long wavelength physics ... breaks at some scale' [32]. Similar to the concept of space-time elasticity the control group explored the relatively stable local physical continuum C in its possible dimensional facets with the prerequisite of knowing the possible location nuclear physic-chemical reactions assisting the astrochemical analysis [33]. The theoretical experiment conducted on the NGC 3034 multi-mission data [12] combined the uses of JS9-4L online34 and SAOImageDS9 on iMac with color mainly coding the local thermal information [27]. Between the control group and experiment group, the conjunction of time anchored to the observer and space and time in objective local universes adopted the shift symmetry and unit weight antisymmetrification theorized by Bonifacio et al. with $T_{\mu\nu} = 1/2 (T_{\mu\nu} - T_{\nu\mu})$, respecting the energy conservation laws of the mechanical systems in an anticipated Collatz conjecture consequences in the parallel experiment group, while preserving the continuity of time with the conjecture stated above [2,21,35].

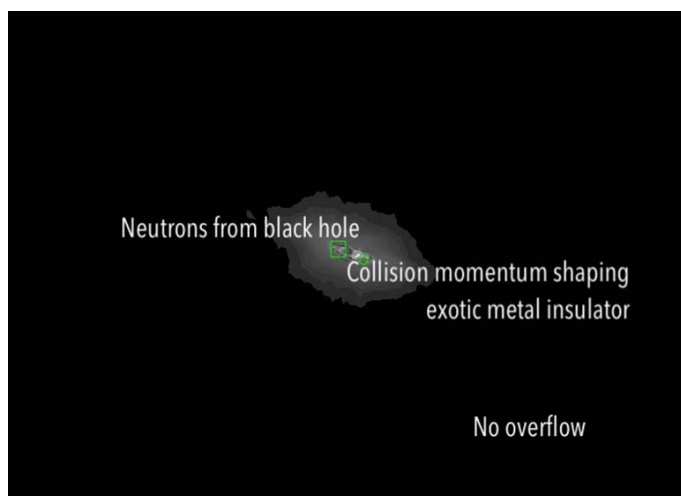


Figure 6: Annotated surface recombination of NGC 3034 anti-matter plasma with neutron signature in the black hole portal (2 visible).

Equation 2 recombined the string theory to a surface plasma analysis through detectable particle signatures distributed in space by diffeomorphism, with figure 6 suggesting a further material twist in the individual antimatter saturated plasma of cold fusion on black hole and hot fission on white hole. The thermally coded color representation on the active galactic nuclei (AGN) generation by the white hole's influence on the black hole on the 0 K ring singularity is seen in figure 7. The randomized experiment group hence partially served for self-cognitive-diagnosis in reducing subjective bias from my theoretical background for a more robust empiricism in the research. With due discretion and multiple sources of confirmation, the theoretical input is expressed in Pachankis [14]:

$$\left\{ S^2 = \left(\frac{\omega r_i \Delta m_2 \pi c^6}{h \nu m_2} \right)^2 \right\}, \quad (5)$$

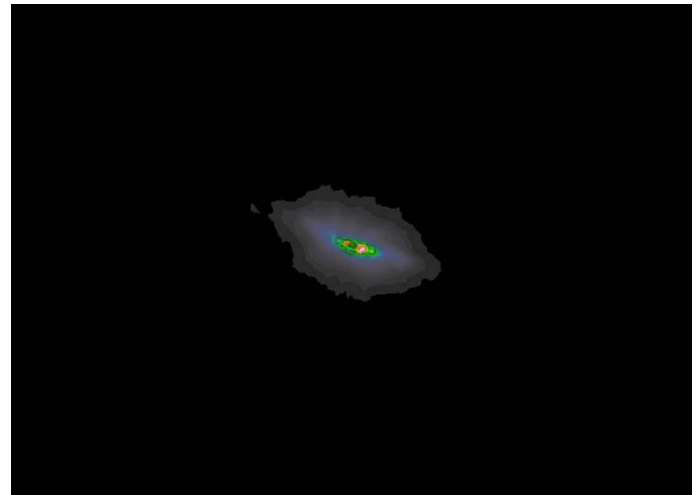


Figure 7: Color-coded plasma analysis with the black hole, white hole, AGN, and quadruple electromagnetic ring.

The antimatter version of the Van der Waals force was experienced by further delving into the white hole gravity inclination in the data [6]. Seen in figure 8, the black hole and white hole are both invisible with a placeholder for the fifth cosmic force binding the two. The neutron decay from the white hole in the asymptotic decay momentum is considered to be the observed gravitation from the multi-mission space telescopes. The symmetric color lines of particle sequences from the decay shows a double-layered sequential pattern. The four dimensions from the momentum are:

- the fifth cosmic force;
- the circular decay sequence;
- the asymmetric lines;
- the vertical axis of the fifth cosmic force.



Figure 8: Annotated asymptotic decay momentum on NGC 3034 with the fifth cosmic force binding the gravitational black hole and white hole.

With the evidence seen in figure 7 and 8, the fifth cosmic force's influence on the C continuum repulses neutrons, therefore, the four dimensions imply two curved planes behind the proton degeneration. The controlled experiment ended with the positive null result with information ample enough in surface wetting of the Kerr-Newman case in black hole, white hole, and the thermonuclear binding force in-between as the fifth cosmic force [4].

Experiment Group

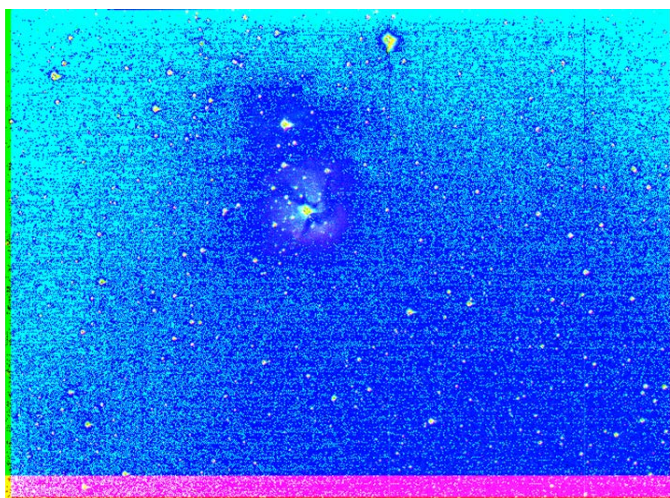


Figure 9: The energy threshold of pulsation on M20 in the observation by the fifth cosmic force [4].

The white hole observations served as a supplement to the possible loss of white hole information in the multi-mission space telescopes for the inherent gravitation effects of instrumentation in space, with nuclear forces behind white holes beyond electrochemistry in the complex Maxwell field and into the antimatter electromagnetism realm [7,12,24,36]. The hypothesis of a negative cosmological constant extended the lengths at the normally presumed low-energy regime in making room for the actually high energy white hole phenomena at the thermonuclear recombination possibilities [7]. The experiment group was conducted on Harvard-Smithsonian MicroObservatory and processed with

JS9-4L online [34]. The moon and sun observations internally validated the other observations of black holes and white holes in galactic scales, by the quadruple impact on the sun and actinic radiation and irradiation from the moon observation [21,37].

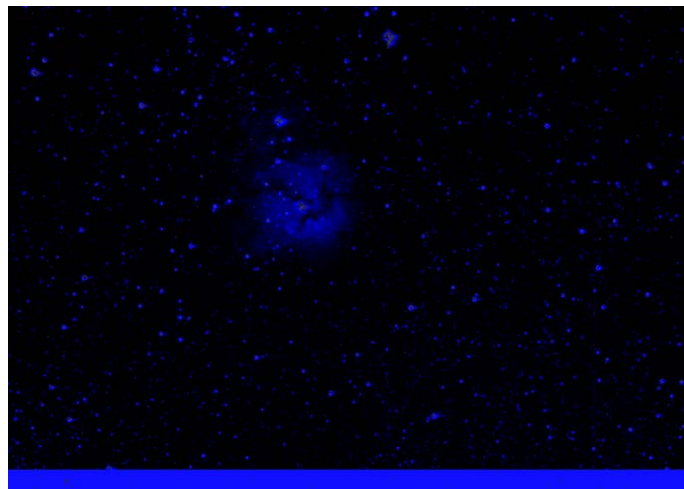


Figure 10: The cold dark matter presentation of the exotic metal insulator on M20 Trifid Nebula.

The M20 Trifid Nebula observation was picked as the focus group in the experiment group, with results of local white hole pulsation observed as predicted [21]. The pulsation effect contributes to the mutual mass gain of black hole and white hole through the accretion phenomenon from the black hole event horizon, but only observable from the white hole portal seen as neutron ejection in proton decay in figure 8. The phenomenon from the pulsation is the volatile cloud formation on the M20 Trifid Nebula seen in figure 9 with further animated details [38]. In the analytic tracing of the crystal body that constitutes the white hole, the same signature of the exotic metal insulator was observed seen in figure 10. The result led to the revisit on the control group with the induction on the exotic metal insulator being neutron rich with the Pauli exclusion principle.

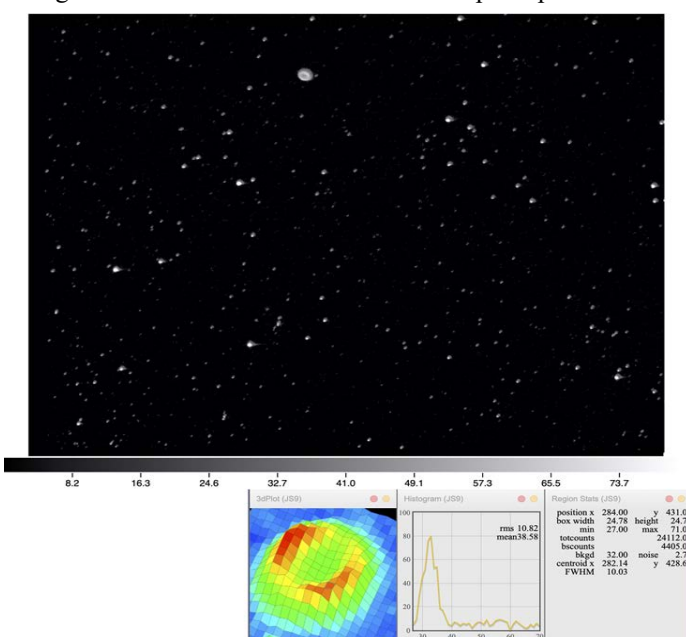


Figure 11: The free-standing graphene wettability phenomenon on the geodesics of the M57 Ring Nebula.

The fusion temperature conduction from the black hole to the white hole raises the surface plasma temperature of the fission process, and theoretically breaks the surface solid matter sedimentation between the fusion plasma and fission plasma. The surface breaking effects in the sequential processing by particle-filtering were observed. The high frequency Doppler Shift in the visual sequence animated thence has been influenced by the quadruple Van der Waals force due to the observation method and instrumentation [38]. The Van der Waals force can be contributed by graphene layers on the ring trajectory seen in figure 11 with freestanding graphene observed in the M57 Ring Nebula, which is less intense than M20 Trifid Nebula [39]. The quantitative evidence from the experiment group observation of the graphene layers in the local sustained thermonuclear collision chains with resonance effects on the star systems imply that the release of dark energy is correlated to the earth's surface plasma's thunder generation, and can be hazardous to outer space assets and earth, creating sudden pressure shifts through atmospheric ionization and earth's intrinsic electromagnetism, if intensified with catalysis. An example can be seen in figure 12 with the Milky Way where white hole seeds signatures were detected with intense energy backlash [40].

Combined with the graphene influence and antimatter electromagnetism on the observational instruments, the thermal phenomenon on the type I and type II Weyl semimetal in the Kedem et al. analysis is explained by the influence of the behavior of light to the electromagnetic wave detection methods [32]. The approximately $-30,000$ Kelvin thermal indicator during the wettability experiment on M20 Trifid Nebula hence can be possibly caused by the energy dispersion effects of graphene materials between the fusion and fission plasma, further increasing the difficulties in more precised detection & observation, apart from the flaring effects from the graphene on the ring trajectories [7,39,41]. The phenomena from the white hole binary on Milky Way imply that the exotic metal insulator can transfer the quadruple matter & antimatter electromagnetic fluxes in energy explosions exacerbated by graphene. The multi-spectral recombination of such effects was processed with the Carina Nebula seen in the cover art.

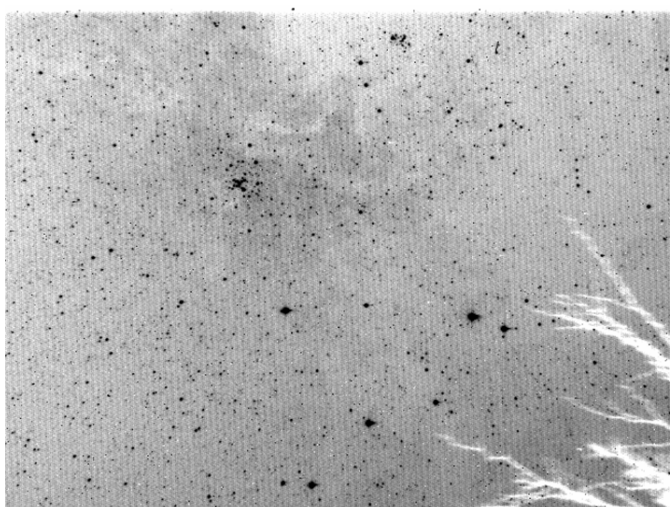


Figure 12: The view from energy backlash shows the white hole seeds trajectories outlines in the Milky Way observation made on Sep 26, 2022.

Results and Discussion

Since the experiments were conducted behind a veil of ignorance on the precise designs and operations of the instrumentation, and the multi-mission space telescopes, the induction on the informatics and computations designs in general relativity implied that the high frequency shift, observed in the experiment group and should exist in NGC 3034, behind the two planes in figure 8, which may be either not captured in the data, or too dangerous to the space based telescopes to explore if there is a robotic artificial intelligence back-end to its operations just as the MicroObservatory in the cybernetics perceived [21,42]. Another possible explanation may be the natural thermonuclear repulsion in outer space acting on the space instrumentation's gravitational fields, composing of the physic-chemical source of cosmic censorship hypothesis.

The spin function observed in histogram was theoretical of the antimatter nuclear electrochemistry in the observed signatures in the black hole and white hole material thermonuclear dynamics, implying four causes of the spin function [12]:

- quadruple electromagnetism around the ring singularity [5];
- spatial pressure of thermonuclear elasticity between the two-body and the ring singularity;
- antimatter electromagnetism's semi-symmetric influence on electrochemical processes in nuclear reactions;
- other external forces' contributions to the focused experiment group, such as intergalactic forces [43].

The control group surface wetting experiment focused on a) and c) as the main contributing factors in the further inductive experimental procedures on the antimatter electromagnetism behaviors in the observed signatures. The surface plasma quadruple electromagnetism of the white hole is reversely correlated to the ring singularity electromagnetism. The thermal pressures provided by the ring singularity quadruple electromagnetism are the condition for the solid formation of the white hole material layers. Albeit the causalities amongst the big bang, black hole formation, and white hole formation are an open epistemological question, the near symmetry of gravitational mass between the black hole and the white hole is almost certain with the surface plasma recombination that made them visible and perceivable. The stability of the structural material states confined by the ring singularity is modulated by the exotic metal-insulator as stabilizer, and the collision momentum implied that the thermonuclear astrochemical reactions around the ring singularity is caused by the black hole and white hole, instead of the other war around, hence led to the preliminary conclusion that the big bang theory is falsified [4].

The plasma irradiation on the surfaces of black hole and white hole implied cold fusion and hot fission processes. The mass formation of the white hole further implied that gaining mass through the fission processes is possible by intermediate antimatter, which contributes to the relatively high surface temperature in hot fission. The thermal conduction mediating the quadruple electromagnetic strengths in the exotic fusion & fission processes may also contribute to the relative stabilities of matter & antimatter clustering in the two masses in the particle

sorting oscillations. The antimatter irradiation in the spins in the Kerr-Newman supermassive compact object is thought to be behind the cause that shapes the black hole and white hole masses through thermonuclear astrochemical processes. Inducted from the fifth cosmic force the exotic metal insulator is supposed to be neutron rich, and stabilizes the gravitational well containing the thermonuclear dynamic masses of the black hole and the white hole [4]. Between the neutron number asymmetry of the black hole and the white hole with the neutron rich exotic metal insulator, the Hawking points are considered as product from the proton decay inside of the fifth cosmic force from the quadruple electromagnetic oscillation in the plasma and with the two masses. The trail of nuclear forces in the local black hole, white hole, and around the fifth cosmic force are conceptually illustrated in the TOC Graphic, and consistent with the cross-examined M87 tails [21,41].

Conclusions

Weinberg predicted the consequences of the proton decay to the cosmological science, and the 'electromagnetic showers ... generated from the decay of neutral pions ... in the nuclear interactions of primary protons' in Perkins's CERN neutrino experiments corroborates with the observational induction. Apart from the muon line of thermonuclear chemical instability in the W-asymmetry in white hole thermonuclear astrochemical stability being corroborated by the laboratory literature the results from figure 8 corroborates with the 'perturbative quantum chromodynamics could be expected to apply' description by Perkins [44,45].

The proton decay momentum shows an electromagnetic parity between the black hole and the white hole interiors with the asymmetric lines. Between figure 8 and 6, the asymmetry of visible neutron numbers observed between the ring trajectories and black and white holes sustains the local astrochemical collision chains. Between the overflow behaviors of NGC 3034 analysis and the high noises in M20 Trifid Nebula, the cleaning of overflow and high noise happened with the surface antimatter plasma recombination and dark matter annihilation, possibly to its anti dark matter counterpart seen in figure 13. Both the control group and experiment group suggest the traditionally perceived low energy domain in proton decay must be associated with antimatter electrolysis, which was also the initial experiment result in 6, treating "low energy" gamma piece in X-ray as high energy with the observation of antimatter distribution on the "event horizon" [12].

From the case of NGC 3034, the counterpart of antimatter electromagnetism parity should lie between protons and neutrons, explaining the binding in radiative process [46]. This is consistent with the thermal phenomenon on the both space and time like singularity on M87 [21,47]. The effects of pulsars in the neutrons thence inductively are caused by the fifth cosmic force with Bremsstrahlung irradiating white hole plasma from black hole plasma [21]. The thermal effects between cold fusion and hot fission brings the neutron-rich overflows to the collision momentum of exotic metal insulator by black hole seeds & white hole seeds, presumably with black hole seeds contributing more to the mass & metallicity of the exotic metal insulator, and white hole thermal effects for consolidation of mass there of.

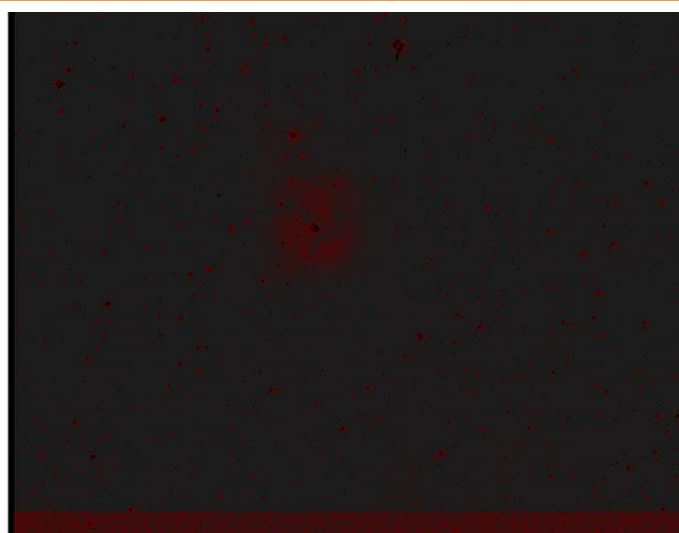


Figure 13: The dark matter annihilation on M20 Trifid Nebula.

The experiment results suggest that neutrons and protons can contain binary antimatter electromagnetism respectively. This may effectively explain the neutron and proton forming a dipion experiment by MASSEY and MOHR resulting with 'a critical frequency below which n is abnormally small, while above it x practically vanishes' [46]. This is contributed by the lack of the extreme intersection elements of both fusion and fission plasma sustaining the critical environment. The asymptotic decay extracts the quadruple electromagnetism from the fifth cosmic force in the material constituents in the Kerr-Newman supermassive compact object case, instead of the normal designs of particle collision. The evidence are not sufficient enough to tell if the fifth cosmic force is monopole from the quadruple electromagnetism, but between proton decay and the product of Hawking points, white hole materials' nuclear chemical bonds may range between the two. The invariance of the Hawking points without apparent crystal flares contributing to absolute magnitude imply that neutron contribution to to surface crystallization in plasma & graphene layers is critical, while the fifth cosmic force's extraction from fusion plasma to white hole material excludes metallicity in the white hole interior materials. The energy preservation effects in white hole mass are contributed by graphene layers in the fission process, filtering out heavier and thicker particle components. From the antimatter Van der Waals force in the proton decay momentum in figure 8, the spin function in the fifth cosmic force determines the evolutionary phases of black-white holes arranged in table 1. Since the main case of NGC 3034 is a star-burst galaxy just as the M20 Trifid Nebula, fission plasma's contribution to the force causing the spins is predominant, while the fusion plasma exerts bonding effects on the fissiling body, further extracting the interior astrochemical bonds of the white hole, causing the primary flare reflected via the crystal body of white hole through the electromagnetic flux in the spectrum. For that the flares cannot be seen from the decay momentum and make the black hole invisible from the electromagnetic spectrum, the fifth cosmic force's repulsive effects on neutrons are evidenced, breaking the parity transformation of the standard model of particle physics, hence the circular lines in figure 8.

Acknowledgement

The author would thanks his parents' support and aunt's support financially regardless of the totalitarian coercion mechanisms of the PRC regime, which preserved the living expenses of the author.

The author also thanks Vicky and Aidan for their Monday astrophotography streams discussing observations and telescopes.

This research is based on observations made with the NASA/ESA Hubble Space Telescope obtained from the Space Telescope Science Institute, which is operated by the Association of Universities for Research in Astronomy, Inc., under NASA contract NAS 5-26555.

This research is based on observations made with the Galaxy Evolution Explorer (GALEX) satellite, a NASA mission led by the California Institute of Technology, obtained from the Space Telescope Science Institute, which is operated by the Association of Universities for Research in Astronomy, Inc., under NASA contract NAS 5-26555.

The scientific results reported in this article are based [in part] on observations made by the Chandra X-ray Observatory.

This work is based [in part] on observations made with the Spitzer Space Telescope, which was operated by the Jet Propulsion Laboratory, California Institute of Technology under a contract with NASA.

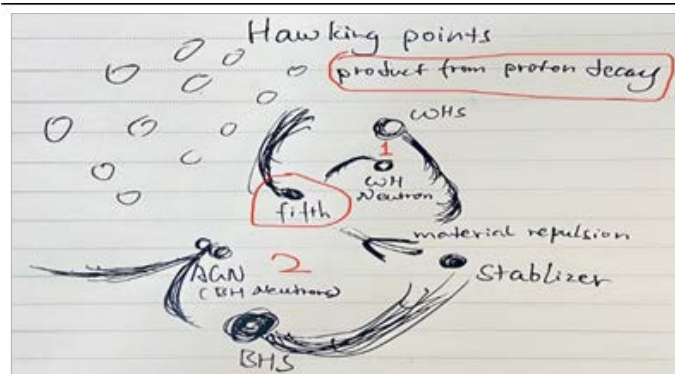
The observations are performed on HarvardSmithsonian Micro-observatory, and the data are processed by JS9-4L online and SAOImageDS9 MacOS.

Supporting Information Available

The data and summary of the initial controlled wettability experiment is openly available in Zenodo at <https://doi.org/10.5281/zenodo.7187684>, and the observational cosmology data experimentally validated the initial results are openly available in Zenodo at <https://doi.org/10.5281/zenodo.7187571>. The data produced from the analysis of the multimission space telescopes' cryogenic plates are openly available in Zenodo at <https://doi.org/10.5281/zenodo.7187733>, and the analysis & re-simulation of the orbital trajectories to the Kerr-Newman supermassive compact object at <https://doi.org/10.5281/zenodo.7188067>, with more detailed results on the gravitational well¹⁸. Recent observations with white hole binary in the Milky Way are openly available in Zenodo at <https://doi.org/10.5281/zenodo.7115842> and the observation on Ring Nebula (M57) with visible black hole seed and white hole seed trajectories openly available in Zenodo at <https://doi.org/10.5281/zenodo.6668133>. The analytic data from the M20 Trifid Nebula observation is openly available in Zenodo at <https://doi.org/10.5281/zenodo.6426887>. The data on the thermal phenomenon on M87 space and like singularity are openly available in Zenodo at <https://doi.org/10.5281/zenodo.6990533>. The initial cosmological force imaging analysis behind the white hole observation series is openly available in Zenodo at <https://doi.org/10.5281/zenodo.6504931>. The quadruple electromagnetic flux on the Carina Nebula behind the cover art

is openly available in Zenodo at <https://doi.org/10.5281/zenodo.6683800>.

TOC Graphic



The trail of nuclear forces in the local black hole, white hole, and around the fifth cosmic force.

References

1. Everett III H (1973) The Many-Worlds Interpretation of Quantum Mechanics; Princeton University Press: Princeton, New Jersey, USA, 1973.
2. Bonifacio J, Hinterbichler K, Joyce A, Roest D (2022) Exceptional scalar theories in de Sitter space. Journal of High Energy Physics 128.
3. Pachankis YI (2021) Research on the Kerr-Newman Black Hole in M82 Confirms Black Hole and White Hole Thermo-nuclear Binding. Academia Letters.
4. Pachankis YI (2022) White Hole on the Horizon of the Fifth Cosmic Force. preprint submitted to New Astronomy.
5. Penrose R (1965) Gravitational Collapse and Space-Time Singularities. Phys Rev Lett 14: 57-59.
6. Pachankis Y (2022) Physical Signals and their Thermo-nuclear Astrochemical Potentials: A Review on Outer Space Technologies*. International Journal of Innovative Science and Research Technology 7: 669-674.
7. Pachankis Y (2022). White Hole Observation: An Experimental Result. International Journal of Innovative Science and Research Technology 7: 779-790.
8. Greene B (1999) The Elegant Universe: Superstrings, Hidden Dimensions, and the Quest for the Ultimate Theory; WW Norton & Company.
9. Brzeminski D, Chacko Z, Dev A, Flood I, Hook A (2022) Searching for a Fifth Force with Atomic and Nuclear Clocks. arXiv e-prints arXiv:2207.14310.
10. Penrose R (2018) The Big Bang and its Dark-Matter Content: Whence, Whither, and Wherefore. Foundations of Physics 48: 1177-1190.
11. Witten, E. Anti-de Sitter space and holography. Advances in Theoretical and Mathematical Physics 1998, 2, 253-291.
12. Pachankis Y (2022) A Multi-wavelength Data Analysis with Multi-mission Space Telescopes. International Journal of Innovative Science and Research Technology 7: 701-708.
13. Pachankis Y (2022) An Evidence-driven Research to the Transgressions of Geneva Conventions by the Communist Party of China Led Autocratic Regime. International Journal of Innovative Science & Research Technology 13.

14. Pachankis Y (2022) Some Concepts of Space, Time, and Lengths in Simplified Chinese* An Analytical Linguistics Approach. International Journal of Innovative Science and Research Technology 7: 550-562.
15. <https://physics.nist.gov/cuu/Units/current.html>.
16. Pachankis YI (2022) Is Time a Physical Unit? preprint submitted to Evolution and Human Behavior.
17. Pachankis YI (2022) Black Hole on Carina Nebula. Zenodo.
18. Ricarte A, Natarajan P (2018) The observational signatures of supermassive black hole seeds. Monthly Notices of the Royal Astronomical Society 481: 3278-3292.
19. Forrington JHC (1972) General Relativity: Effects in Time as Causation. Journal of Modern Cosmology 1: 31.
20. Pachankis YI (2021) Theoretical and Controlled Wettability Experiment on NGC 3034 with Photochemistry in Quantum.
21. Pachankis YI (2022) The Lenses of Quantum Physics on Earth to the Cosmos: From the Humanities to the Apocalyptic Inevitability; Eliva Press: Moldova, Europe, Chapter 8, pp 237-345.
22. Poincaré H (1907) The Value of Science; The Science Press, 1907; Chapter IV, p 55.
23. Bothun G, Impey C, McGaugh S (1997) Low-Surface-Brightness Galaxies: Hidden Galaxies Revealed. Publications of the Astronomical Society of the Pacific 109: 745.
24. Hawking SW, Perry MJ, Strominger A (2016) Soft Hair on Black Holes. Physical Review Letters 116: 231301.
25. Pachankis Y (2022) Reading the Cold War through Outer Space: The Past and Future of Outer Space. International Journal of Scientific & Engineering Research 13: 826-829.
26. Bodendorfer N, Mele FM, Münch J (2021) Mass and horizon Dirac observables in effective models of quantum black-to-white hole transition. Classical and Quantum Gravity 38.
27. Joye W (2019) SAO Image DS9/SAO Image DS9 v8.0.1.
28. Lindahl, Abraham, Hess, van der Spoel (2020) GROMACS 2019.6 Manual.
29. Iqbal M, Dinh DK, Abbas Q, Imran M, Sattar H, ET AL. (2019) Controlled Surface Wettability by Plasma Polymer Surface Modification. Surfaces 2: 349-371.
30. Pachankis YI (2022) Mass Surveillance, Behavioural Control, And Psychological Coercion - The Moral Ethical Risks in Commercial Devices. Computer Science and Information Technology 151-168.
31. Kant I (1781) Critique of Pure Reason.
32. Kedom Y, Bergholtz EJ, Wilczek F (2020) Black and white holes at material junctions. Phys Rev Research 2: 043285.
33. Challoumis C (2021) Singularity Universe or Parallel Universes? - MSP Theory (Multiple Singular and Parallel Theory). Available at SSRN.
34. Ferland GJ, Porter RL, van Hoof PAM, Williams RJR, Abel NP, et al. (2013) The 2013 Release of Cloudy. Revista Mexicana de Astronomía y Astrofísica, 49: 137-163.
35. Challoumis C (2019) Creation Theory The Light Space, the Dimensional Space and the Bounded Infinities - Where Comes the Energy of Multiple Big Bangs? Available at SSRN.
36. Pachankis Yang (2021) White Hole Observation experiment.
37. Pachankis Yang (2021) Black Hole and White Hole Time Dilation
38. Pachankis YI (2021) White Hole on the Trifid Nebula.
39. Belyaeva LA, Schneider GF (2020) Wettability of graphene. Surface Science Reports 75: 100482.
40. Pachankis YI (2022) Revisiting the Milky Way — White Hole Binary with Energy Backlash and White Hole Seed Signature.
41. Event Horizon Telescope Collaboration, Kazunori Akiyama, Anton Alberdi, Walter Alef, Keiichi Asada, Rebecca Azulay, et al. (2019) First M87 Event Horizon Telescope Results. V. Physical Origin of the Asymmetric Ring. The Astrophysical Journal Letters 875: L5.
42. Pachankis Y (2022) Technical Analysis on the Cyber Organizational Criminology of Dictatorial Military Conducts Experience from Human Trafficking and Coercions by Military Cyber Aggressions. International Journal of Security 11: 1.
43. <https://sites.psu.edu/rdaly/476-2/>.
44. Weinberg S (1981) The Decay of the Proton. Scientific American 244: 64-75.
45. Perkins DH (2005) From Pions to Proton Decay: Tales of the Unexpected. Annual Review of Nuclear and Particle Science 55: 1-26.
46. Massey HSW, Mohr CBO (1934) Radiative Collisions of Neutrons and Protons. Nature 133: 211.
47. Pachankis YI (2021) VirgoA M87 Heat Transfer. Zenodo.